Am J Transl Res 2026;18(6):5468-5476
www.ajtr.org /ISSN:1943-8141/AJTR0173340

Original Article

Novel desktop robotic system for orthodontic archwire bending: an accuracy and efficiency comparison with manual bending

Chenyang Qiu, Hongcheng Xing, Jiaxiang Zhang, Shiyi Liu, Xinyi Liu, Dongliang Zhang

Department of Orthodontics, Beijing Stomatological Hospital, Capital Medical University, Beijing 100070, China

Received April 15, 2026; Accepted June 18, 2026; Epub June 25, 2026; Published June 30, 2026

Abstract: Purpose: To determine whether the bending accuracy and operational efficiency of a newly-developed desktop robotic archwire-bending system outperform manual bending performed by an experienced orthodontist. Methods: A customized lingual orthodontic archwire with 9 bending nodes and two linear dimensional parameters (width and height) was set as the target specimen. Comparative tests were conducted using 0.5 mm round stainless steel archwires. Specimens were divided into robot and manual groups, with 12 replicates tested for each group. The robot group performed bending according to a three-dimensional (3D) stereolithography (STL) model of the target archwire, while all manual bending operations were completed by a single attending orthodontist. High-resolution two-dimensional images of finished archwires were captured, and angular and linear bending deviations were quantified by image analysis software. Bending duration was recorded using a stopwatch. Results: The robot group exhibited significantly smaller deviations in three angular parameters and the height parameter than the manual group (P<0.05). No significant intergroup differences were found for the remaining six angular parameters and the width parameter (P=0.053). The mean bending time was 141.0±10.2 seconds for the robot group, nearly 45% of the manual group's duration (316.1±36.2 seconds), and this time difference was statistically significant (P<0.05). Conclusions: The proposed desktop robotic system achieves accuracy comparable to skilled orthodontists for most bending parameters, with superior precision in specific angular indices and vertical height. Additionally, the robotic system delivered faster, more efficient and highly consistent archwire bending performance.

Keywords: Orthodontics, archwire bending, industrial robot, dimensional accuracy, operational efficiency, digital dentistry

Introduction

Orthodontic archwire bending is an indispensable procedure in fixed orthodontic treatment. A well-contoured archwire must perfectly match the patient's 3D dental arch morphology to deliver predetermined orthodontic forces precisely [1, 2]. Clinically conventional manual bending relies entirely on visual judgment and handheld bending pliers. This approach suffers from poor dimensional accuracy and strong operator dependence. Manual bending errors are exacerbated by the intrinsic springback property of metallic archwires and the complexity of multi-planar bending geometry [3-5]. Intra-operator and inter-operator measurement discrepancies inevitably occur during repeated manual fine-tuning, further amplifying morphologic deviations of bent segments. Iterative manual adjustment also causes localized surface abrasion and structural distortion of archwires, and repeated plastic deformation alters the archwire's intrinsic mechanical properties [6]. Beyond dimensional errors, prolonged manual bending increases clinician physical fatigue and extends patient chairside waiting time, hindering overall workflow efficiency.

To reduce reliance on manual operative skills, alleviate clinician workload, and promote digital and automated orthodontic workflows, robotic archwire bending has been proposed as an alternative clinical solution [7, 8]. Robotic systems demonstrate superior repeat positioning accuracy and faster displacement response compared to manual operations, while eliminat-

https://doi.org/10.62347/BIVN7584

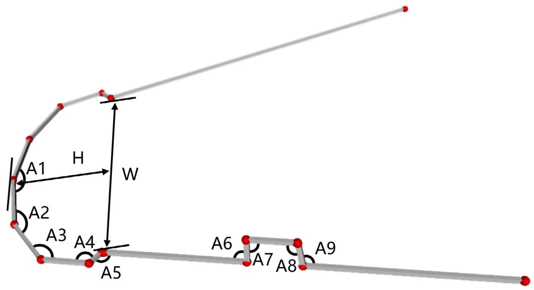

Figure 1. Target archwire shape and parameter definitions.

ing human-induced operational error. Multiple archwire-bending robotic prototypes have been reported in prior literature [9, 10]. The LAMDA system was designed exclusively for planar lingual archwire bending and lacks vertical bending functionality, limiting its clinical applicability [11]. Another prototype based on the MOTOMAN UP6 robotic arm optimized bending velocity and angular parameters for first-order planar bends only. The SureSmile system, a mature commercial digital orthodontic platform, integrates 3D intraoral scanning, treatment simulation and robotic customized archwire fabrication with proven clinical efficacy [12, 13]. However, widespread clinical adoption of existing robotic systems is hindered by unresolved springback compensation defects, bulky structural volume, and high procurement and maintenance costs [14]. There remains an unmet clinical need for compact, low-cost, user-friendly high-precision desktop archwire-bending robots.

This study introduces a novel compact desktop archwire-bending robotic system. Unlike conventional multi-degree-of-freedom articulated robotic arms, this prototype adopts a planar modular structure consisting of independent wire feeding and bending units, with only five functional degrees of freedom including the clamping mechanism. It retains the capability of fabricating complex 3D archwire geometries while lowering manufacturing costs and reducing footprint for routine clinical use. The two primary research objectives were: (1) To elaborate the mechanical design and closed-loop control strategy of the proposed robotic system; (2) To compare the bending accuracy and operational efficiency between the robotic system and manual bending performed by an experienced orthodontist.

Table 1. Target values of key archwire bending parameters

Parameter	Target value
A1	163.1°
A2	155.5°
A3	137.7°
A4	117.4°
A5	117.9°
A6	90.0°
A7	90.0°
A8	90.0°
A9	90.0°
W	27.26 mm
H	11.24 mm

H, vertical height; W, transverse width; A1-A9, bending angles at nodes 1-9.

Materials and methods

Experimental design and system configuration

Both robotic and manual workflows targeted identical lingual archwire geometries containing combined first-order and second-order multi-planar bends (**Figure 1**). Measured values included nine bending angles (A1-A9), transverse width and vertical height, with theoretical reference values extracted from the validated 3D archwire STL model (**Table 1**). Test specimens were fabricated using 0.5 mm round stainless steel archwires (Suhang Wire Industry Co., Ltd., Shenzhen, China), a mainstream clinical material with stable elastic modulus and reliable plastic formability.

For the robotic group, archwires were bent automatically after importing the standardized 3D STL model into the robotic control system. For the manual group, all bending operations were performed by a single orthodontist with 15 years of clinical experience, who strictly followed the reference dimensional parameters and 3D geometric diagrams. Twelve independent archwire specimens were fabricated for each group.

The core robotic hardware comprised integrated wire feeding and bending modules (**Figures 2**, **3**). The wire feeding module contained a pneumatic clamping fixture and servo drive motor, which precisely controlled linear wire advancement and axial end rotation (90° or

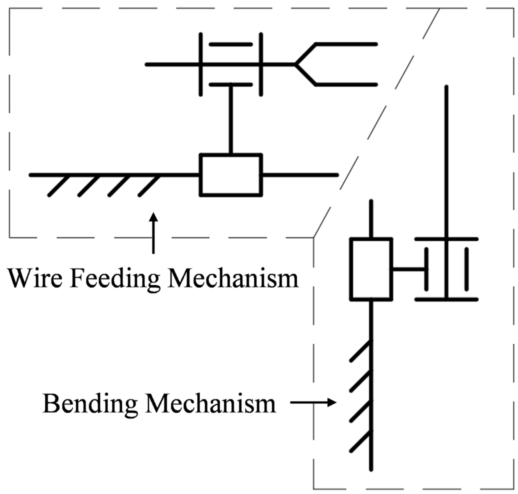

Figure 2. A schematic diagram of the wire-fed-and-bending mechanism for the robot system.

180°) to align archwires for first-order, second-order and vertical bending planes.

The bending module consisted of a fixed hollow die and a rotating eccentric die. Traditional paired parallel dies require strict axial alignment and occupy excessive spatial volume. The hollow fixed die used in this study achieves stable circumferential wire clamping without redundant alignment calibration. The rotating die pivots around the fixed die to generate bending torque, and its flat top surface enables integrated archwire cutting after bending completion. The rotating die was connected to a stepping motor through a rigid coupling for torque transmission. The stepping motor and rotating die were mounted on a vertical linear slide module to realize automatic tool retraction during wire cutting (**Figure 3**).

Wire springback compensation strategy

The robotic control program integrates 3D path planning and material-specific springback compensation. Metallic archwires undergo elastic springback after torque unloading, creating deviations between programmed and actual bending angles. To mitigate this error, preliminary springback quantification tests were conducted on 0.5 mm stainless steel archwires across incremental bending angles. Collected springback datasets were fitted through fifth-order polynomial regression to establish a predictive springback compensation model embedded in the robotic control algorithm.

Robotic archwire bending workflow

After importing the target archwire STL file, the system automatically calculated feeding distance, bending angle, rotational direction, and springback compensation offset. The robot sequentially executed wire feeding, axial rotation and torque bending according to optimized path parameters without manual intermediate intervention (**Figure 4**).

Parameter calibration and outcome evaluation

Finished archwires were placed horizontally on a vibration-free optical platform. Two orthogonal sets of high-resolution 2D images were captured vertically with a calibrated digital camera, with a standard vernier ruler affixed for pixel-scale dimensional calibration (**Figure 5**). Images were imported into Image Measuring Software V6.0 for angular and linear deviation measurement. All measurements were completed by one blinded orthodontist with no access to group allocation information. Each parameter was measured in triplicate, and mean values were used for statistical analysis.

Bending duration was recorded using an electronic stopwatch. Robotic bending time was defined as the interval from STL model import to full archwire fabrication and cutting. Manual bending time covered the period from initial wire clamping to final geometric adjustment by the orthodontist.

All archwire blanks were sourced from a single production batch to eliminate material heterogeneity. Surface Vickers hardness was tested at three randomly selected points on each blank using an HVS-1000 microhardness tester under a 200 g indentation load for 10 seconds. No surface polishing or cleaning was performed prior to testing to preserve original material properties.

Secondary outcome indicators included total contour length deviation, straight segment flatness and surface morphologic quality. Total contour length deviation referred to the absolute difference between the actual central line length traced via image software and the theoretical length derived from the STL model.

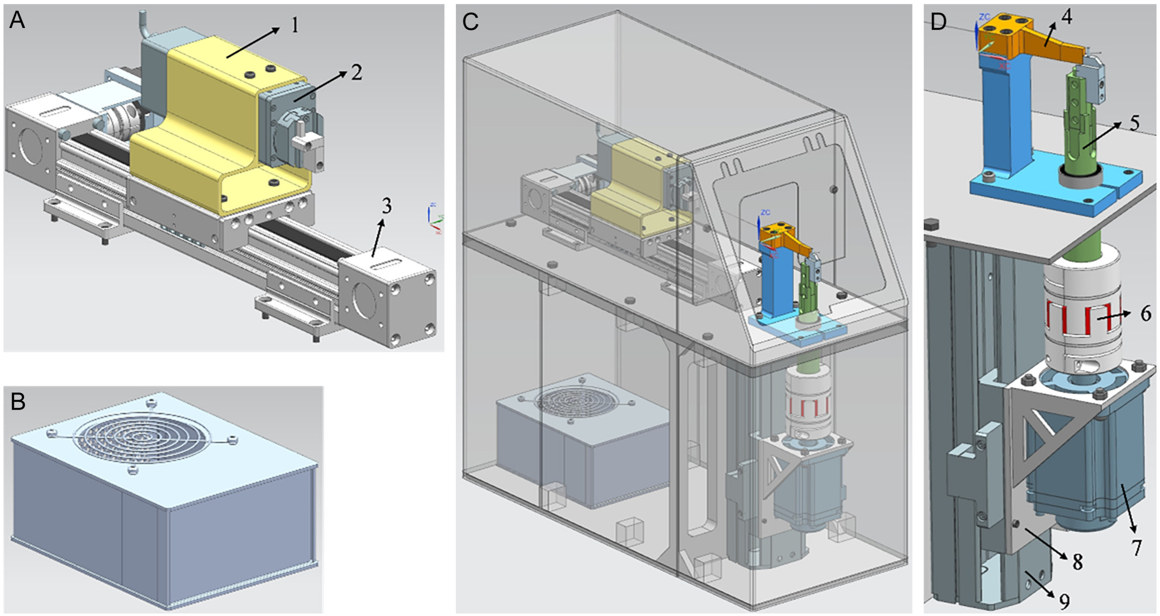

Figure 3. Explored view of the desktop robotic system assembly. A. Wire-feeding mechanism: A-1. Mounting bracket, A-2. Motorized rotary gripper, A-3. Synchronous belt linear drive module; B. Power supply unit; C. Schematic diagram of the overall structural layout; D. Bending mechanism: D-4. Fixed die, D-5. Rotating die, D-6. Coupling, D-7. Stepper motor, D-8. Stepper motor mount, D-9. Linear motor.

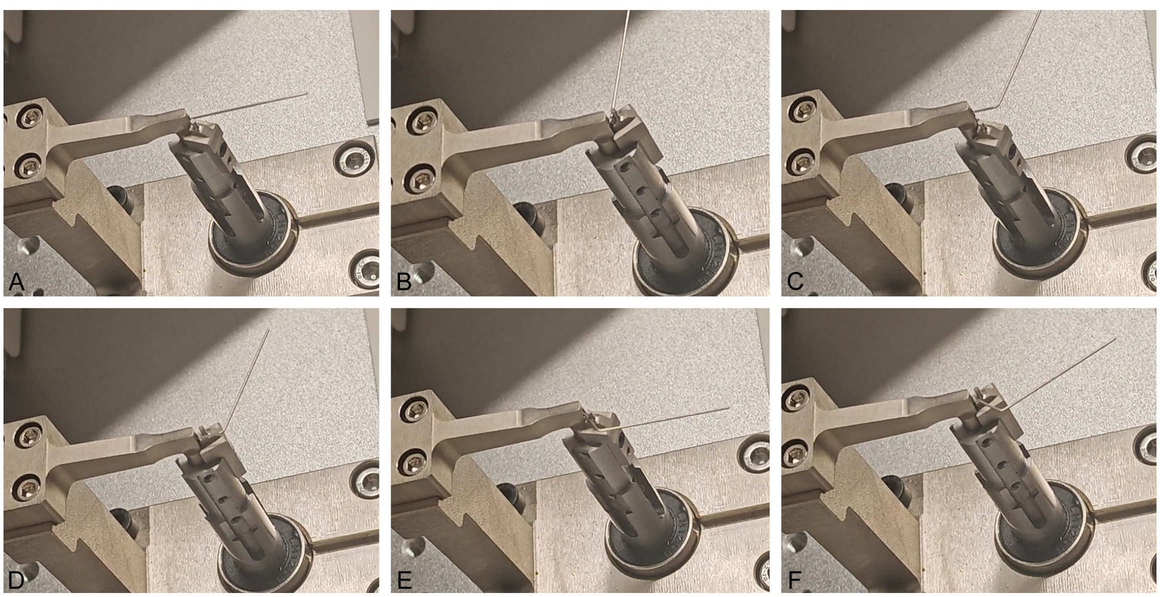

Figure 4. Bending process for an archwire bending robot system. A-C. Left bending process: The rotating die is positioned on the right side of the archwire and rotates counterclockwise to perform the left bend; D-F. Right bending process: The rotating die is positioned on the left side of the archwire and rotates clockwise to perform the right bend.

Straight segment flatness was quantified as the standard deviation of vertical offset for each linear archwire segment relative to the horizontal reference plane. Surface quality was independently scored by two blinded assessors under standardized white light with 2.5× magnifying loupes using a 5-point scale (5 = no visible scratchesand 1 = severe structural

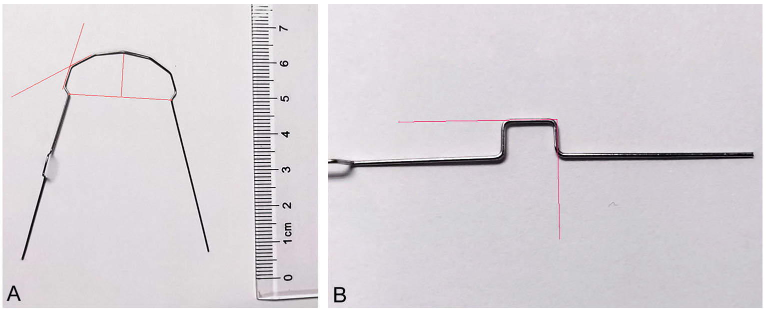

Figure 5. The angle and distance parameters measured in archwire photographs using digimizer software. A. Photograph taken perpendicular to the first-order bends, with a millimeter ruler as a size reference to calibrate the deviation between the image and the actual dimensions; B. Photograph taken perpendicular to the second-order bends.

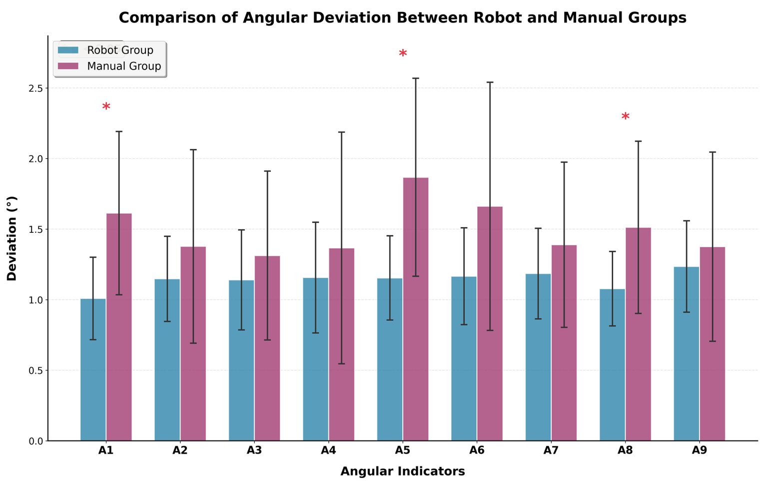

Figure 6. Deviation of bending angles between the two groups.

abrasion). Inter-assessor mean scores were adopted for statistical analysis.

Statistical analysis

All statistical analyses were performed using IBM SPSS Statistics 17.0. Data were reported as means, standard deviations (SD), minimum/maximum values, and 95% confidence intervals (CIs). The sample size of 12 specimens per group was determined based on prior orthodontic bending literature and preliminary pilot tests, rather than prospective power calculation. The Shapiro-Wilk test was used to verify data normality. Normally distributed data were compared by independent-samples t-tests, while non-normal data were analyzed using the Mann-Whitney U test. Given 11 pairwise parameter comparisons, the Bonferroni method was applied to correct type I error, yielding an adjusted significance threshold of P=0.0045. Consistent with exploratory study reporting conventions, uncorrected *p*-values are presented in the results, with the corrected threshold noted for interpretation. A raw *p*-value <0.05 was defined as significant.

Results

Overall angular bending accuracy

All 12 bending replicates were successfully completed in both groups with no archwire fracture. Both groups achieved satisfactory overall angular bending accuracy. Statistically significant angular deviations were detected in three of nine bending nodes (P<0.05; **Figure 6**), with no intergroup differences for the remaining six angles. After Bonferroni correction, these three angular differences and vertical height deviation remained significant, confirming robust results (**Tables 2**, **3**).

Basic material properties and secondary morphologic outcomes

Pre-bending surface hardness showed no significant intergroup difference (P>0.05), confirming consistent initial material properties across test groups (**Table 4**). Secondary morphologic outcomes were comparable between groups: total contour length deviation and straight segment flatness exhibited no statistical differences (P>0.05). Mean surface quality scores were 4.33±0.51 for the robot group and 4.15±0.60 for the manual group (P=0.450), indicating equivalent surface abrasion levels for the two bending methods (**Table 5**).

Linear dimensional deviation of archwires

For linear dimensional deviations, transverse width deviation was 1.39±0.17 mm (robot

Table 2. Formed deviation using robotic system

Deviation	Max	Min	Mean	SD	95% CI	
					Lower	Upper
A1 (°)	1.48	0.5	1.01	0.29	0.82	1.19
A2 (°)	1.7	0.67	1.15	0.30	0.96	1.34
A3 (°)	1.82	0.63	1.14	0.35	0.91	1.37
A4 (°)	2.06	0.68	1.16	0.39	0.91	1.41
A5 (°)	1.75	0.72	1.15	0.30	0.96	1.34
A6 (°)	1.84	0.64	1.17	0.34	0.95	1.38
A7 (°)	1.82	0.63	1.19	0.32	0.98	1.39
A8 (°)	1.43	0.31	1.04	0.32	0.91	1.25
A9 (°)	1.91	0.72	1.24	0.32	1.03	1.44
W (mm)	1.67	1.06	1.39	0.17	1.28	1.50
H (mm)	1.27	0.63	0.96	0.18	0.84	1.08

H, vertical height; W, transverse width; A1-A9, bending angles at nodes 1-9.

Table 3. Formed deviation of manual group

Deviation	Max	Min	Mean	SD	95% CI	
					Lower	Upper
A1 (°)	2.72	0.67	1.61	0.58	1.25	1.98
A2 (°)	2.71	0.25	1.38	0.69	0.94	1.81
A3 (°)	2.35	0.19	1.31	0.60	0.93	1.69
A4 (°)	2.92	0.04	1.37	0.82	0.85	1.89
A5 (°)	2.92	0.73	1.87	0.70	1.42	2.31
A6 (°)	3.37	0.44	1.66	0.88	1.10	2.22
A7 (°)	2.33	0.26	1.39	0.59	1.02	1.76
A8 (°)	2.43	0.46	1.50	0.55	1.15	1.85
A9 (°)	2.52	0.23	1.38	0.67	0.95	1.80
W (mm)	3.28	0.63	1.89	0.78	1.39	2.38
H (mm)	2.54	0.61	1.57	0.59	1.19	1.95

H, vertical height; W, transverse width; A1-A9, bending angles at nodes 1-9.

Table 4. Baseline characteristics of archwire samples before bending

Measurement	Robot Group (n=12)	Manual Group (n=12)	t	P
Surface hardness (HV0.2)	245.33±4.25	246.15±3.91	0.489	0.630

Table 5. Secondary geometric and surface quality results after bending

Measurement	Robot Group (n=12)	Manual Group (n=12)	t	P
Total length deviation (mm)	1.22±0.35	1.48±0.62	1.293	0.209
Straight segment flatness (mm)	0.14±0.05	0.17±0.07	1.378	0.182
Surface quality score (1-5)	4.33±0.51	4.15±0.6	0.769	0.450

group) versus 1.89±0.78 mm (manual group), with a marginal non-significant difference (P=0.053). Vertical height deviation was 0.96±0.18 mm in the robot group and 1.57±0.59 mm in the manual group, representing a significant improvement for robotic bending (P<0.05; **Figure 7**).

Operational efficiency of bending operation

The robotic system demonstrated substantial time efficiency gains. Mean fabrication time was 141.0±10.2 s for robotic bending and 316.1±36.2 s for manual bending, with robotic operations consuming only 44.6% of manual working time (P<0.05, **Table 6**).

Discussion

Archwire bending bridges digital tooth movement planning and chairside orthodontic implementation. Traditionally, this procedure requires years of specialized clinician training and prolonged chairside operation, yet manual workflows cannot guarantee consistent geometric accuracy [15]. This study quantitatively compared accuracy and efficiency between a novel desktop robotic system and expert manual bending, addressing limitations of prior single-factor robotic tests lacking controlled human-group comparisons [16-18].

The accuracy gap between manual and robotic bending stems from fundamental positioning logic differences. Manual bending relies on naked-eye visual estimation and iterative handheld measurement, which are inherently prone to subjective human error and low repeatability [3]. In contrast, the robotic system executes displacement based on calibrated 3D digital coordinates with a static positioning tolerance of

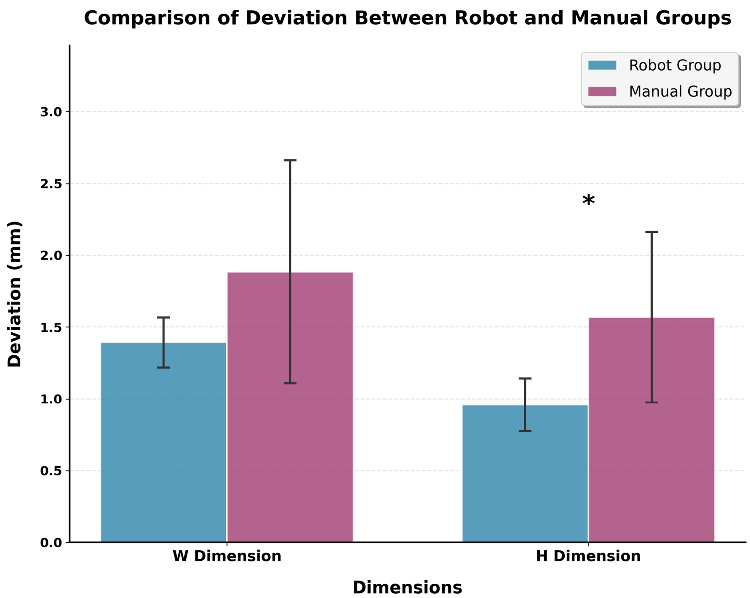

Figure 7. Comparison of distance errors in the two groups.

Table 6. Time required for archwire bending

Time	Max	Min	Mean	SD	95% CI	
					Lower	Upper
Robot	159	124	141.0	10.2	134.5	147.5
Manual	373	252	316.1	36.2	293.1	339.1

±0.01 mm and stable long-term operational output [19-21]. Embedded material-specific springback compensation further improves post-bending geometric accuracy. The fifth-order polynomial compensation model offsets elastic recovery before bending execution, avoiding post-bending manual readjustment. This finding aligns with existing studies verifying that proactive springback compensation reduces angular bending errors in robotic archwire fabrication [13, 22].

Single-pass compensated robotic bending minimizes repeated plastic deformation of archwires [23, 24]. Multiple manual readjustments induce cumulative material fatigue: Tian et al. [6] verified that three or more repeated bending cycles reduce archwire flexural stiffness and torque output, while four cycles significantly increase fracture risk. Robotic single-pass forming avoids such mechanical degradation and preserves intrinsic archwire biomechanical properties.

The differential accuracy performance across parameters reflects distinct error accumulation mechanisms. The robotic system delivered superior precision for three localized bending angles due to stable torque control, while matching manual accuracy for the remaining six angles. Transverse width represents cumulative error across sequential multi-point bends: microscopic angular deviations at individual nodes accumulate along the horizontal axis, offsetting single-point robotic precision advantages [25, 26]. Manual bending, by contrast, produces systematic errors that clinicians partially correct subconsciously during iterative adjustment, narrowing overall width deviation gaps. The robotic system's stable error distribution is better suited for standardized batch archwire production than subjective manual adjustment [22, 27, 28].

All observed dimensional deviations fell within clinically acceptable thresholds. The robotic height deviation accounted for 8.5% of the theoretical target height, and width deviation accounted for 5.1% of theoretical target width. Minor vertical and transverse archwire discrepancies can be compensated by bracket slot engagement and ligature adjustment during clinical bonding, and do not alter the magnitude or direction of orthodontic force delivery. Accordingly, the statistically significant height deviation advantage of the robot does not translate to meaningful clinical performance differences.

The robotic time efficiency advantage originates from automated feeding and integrated bending-cutting workflows. Manual bending requires repeated template comparisons, dimensional measurement, and corrective fine-tuning, which prolongs operation time. The robotic system completes wire positioning, rotation, bending, and cutting autonomously without human auxiliary alignment, eliminating redundant manual steps [29, 30].

Modular mechanical design is the core advantage of the proposed desktop robot. By splitting feeding and bending degrees of freedom, the system avoids redundant articulated joints that cause cumulative positioning errors in multi-axis robotic arms. Simplified mechanical structures reduce equipment volume and manufacturing costs, adapting to limited chairside workspace in dental clinics.

This study has four key limitations. First, tests were limited to 0.5 mm round stainless steel archwires and one lingual archwire geometry. Nickel-titanium and beta-titanium archwires exhibit divergent springback characteristics, requiring targeted compensation model revision for future application. Second, manual bending was performed by only one clinician, so inter-operator variability in manual accuracy was not evaluated. Third, all tests were conducted *in vitro*; clinical outcomes including archwire fitting and patient comfort remain unvalidated. Fourth, sample size was determined empirically rather than by prospective power analysis, introducing possible sampling bias.

Conclusions

The novel desktop archwire-bending robotic system achieves equivalent accuracy and superior operational stability compared to experienced orthodontists. Its compact footprint, low manufacturing cost and user-friendly workflow support widespread chairside clinical deployment. Future research should expand test material types, validate personalized archwire fitting performance, conduct prospective clinical trials and optimize sample size design. With the maturation of digital orthodontic technology, this compact robotic system will support closed-loop digital workflows from virtual treatment planning to accurate execution.

Acknowledgements

This study was supported by the Capital's Funds for Health Improvement and Research (No. 2024-2-2143).

Disclosure of conflict of interest

None.

Address correspondence to: Dongliang Zhang, Department of Orthodontics, Beijing Stomatological Hospital, Capital Medical University, No. 9 Fanjiacun Road, Fengtai District, Beijing 100070, China. E-mail: zhangdongliang5718@163.com

References

[1] Chainani P, Paul P and Shivlani V. Recent advances in orthodontic archwires: a review. Cureus 2023; 15: e47633.
[2] Alemran MA, Abbassy MA and Zawawi KH. Frictional resistance in orthodontic archwires: a comprehensive review. J Orthod Sci 2025; 14: 43.
[3] Ahmad P, Alam MK, Aldajani A, Alahmari A, Alanazi A, Stoddart M and Sghaireen MG. Dental robotics: a disruptive technology. Sensors (Basel) 2021; 21: 3308.
[4] George BM, Arya S, G S S, Bharadwaj K and N S V. Robotic archwire bending in orthodontics: a review of the literature. Cureus 2024; 16: e56611.
[5] Liu L, Watanabe M and Ichikawa T. Robotics in dentistry: a narrative review. Dent J (Basel) 2023; 11: 62.
[6] Tian S, Dai J, Ahmad W, Liang K, Tan Q, Deng H, Jiang F, Xiong J, Cao J and Xia Z. Mechanical effect of different patterns for preparation of orthodontic appliances: an experimental study. Dent Mater J 2024; 43: 637-642.
[7] Adel S, Zaher A, El Harouni N, Venugopal A, Premjani P and Vaid N. Robotic applications in orthodontics: changing the face of contemporary clinical care. Biomed Res Int 2021; 2021: 9954615.
[8] Seidel CL, Lipp J, Dotzer B, Janjic Rankovic M, Mertmann M, Wichelhaus A and Sabbagh H. Investigation of forces and moments during orthodontic tooth intrusion using robot orthodontic measurement and simulation system (ROSS). Bioengineering (Basel) 2023; 10: 1356.
[9] Sabbagh H, Haas E, Baumert U, Seidel CL, Hötzel L and Wichelhaus A. Biomechanical simulation of orthodontic en-bloc retraction comparing compound technique and sliding mechanics using a HOSEA robotic device. Bioengineering (Basel) 2024; 11: 153.
[10] Dotzer B, Stocker T, Wichelhaus A, Janjic Rankovic M and Sabbagh H. Biomechanical simulation of forces and moments of initial orthodontic tooth movement in dependence on the used archwire system by ROSS (Robot Orthodontic Measurement & Simulation System). J Mech Behav Biomed Mater 2023; 144: 105960.
[11] Gilbert A. An in-office wire-bending robot for lingual orthodontics. J Clin Orthod 2011; 45: 230-234; quiz 236.
[12] Millesi GA, De Fazio GR, Zimmermann M and Eltz M. Improved stability of open bite deformi-

ties: taking control of the transverse width using digital technology and robotic archwire bending. Int J Oral Maxillofac Surg 2025; 54: 245-250.
[13] Liu H, Jiang J, Wang J, Zhou S, Zhang Y and Liu S. A review of the research progress of orthodontic archwire bending robot for fixed appliances. IEEE Access 2024; 12: 167638-167654.
[14] Sabbagh H, Dotzer B, Baumert U, Hötzel L, Seidel CL and Wichelhaus A. Biomechanical simulation of segmented intrusion of a mandibular canine using robot orthodontic measurement & simulation system (ROSS). J Mech Behav Biomed Mater 2024; 160: 106720.
[15] De La Garza-Ramos MA, Ipiña-Lozano HH, Cano-Verdugo G, Nakagoshi-Cepeda MAA and Liu Y. Application of robotics in orthodontics: a systematic review. Cureus 2024; 16: e58555.
[16] Tian YN, Li BX, Zhang H and Jin L. Development of dental robot implantation technology. Zhonghua Kou Qiang Yi Xue Za Zhi 2023; 58: 1300-1306.
[17] Fawaz P, El Sayegh P and Vande Vannet B. Artificial intelligence in revolutionizing orthodontic practice. World J Methodol 2025; 15: 100598.
[18] Bahrami R, Pourhajibagher M, Nikparto N and Bahador A. Robot-assisted dental implant surgery procedure: a literature review. J Dent Sci 2024; 19: 1359-1368.
[19] Yao L, Jiang J, Zhang Y, Wang J, Zhou S and Liu Y. Orthodontic force/torque modeling and experiment of Kitchon root-controlled auxiliary archwire. Int J Numer Method Biomed Eng 2024; 40: e3789.
[20] Terzi M, Yavuz MC, Bicer T and Buyuk SK. Evaluation of artificial intelligence robot's knowledge and reliability on dental implants and peri-implant phenotype. Sci Rep 2025; 15: 9519.
[21] Jiang JG, Han YS, Zhang YD, Liu YJ, Wang Z and Liu Y. Springback mechanism analysis and experiments on robotic bending of rectangular orthodontic archwire. Chin J Mech Eng 2017; 30: 1406-1415.
[22] Jiang J, Ma X, Zuo S, Zhang Y and Liu Y. Digital expression and interactive adjustment method of personalized orthodontic archwire for robotic bending. J Adv Mech Des Syst Manuf 2019; 13: JAMDSM0031.
[23] Fawaz P, Sayegh PE and Vannet BV. What is the current state of artificial intelligence applications in dentistry and orthodontics? J Stomatol Oral Maxillofac Surg 2023; 124: 101524.
[24] Alessa N. Application of artificial intelligence in pediatric dentistry: a literature review. J Pharm Bioallied Sci 2024; 16 Suppl 3: S1938-S1940.
[25] Swain SK, Sahu PK, Jena BR and Acharya B. Emerging applications of medical nanorobots in health care: current trends and future prospects. Curr Mol Med 2025; 25: 1231-1251.
[26] On SW, Cho SW, Park SY, Yi SM, Park IY, Byun SH, Kim JC and Yang BE. Advancements in computer-assisted orthognathic surgery: a comprehensive review and clinical application in South Korea. J Dent 2024; 146: 105061.
[27] Olawade DB, Leena N, Egbon E, Rai J, Mohammed APEK, Oladapo BI and Boussios S. AI-driven advancements in orthodontics for precision and patient outcomes. Dent J (Basel) 2025; 13: 198.
[28] Li Y, Inamochi Y, Wang Z and Fueki K. Clinical application of robots in dentistry: a scoping review. J Prosthodont Res 2024; 68: 193-205.
[29] Kim Y, Kumar RS and Kim J. Medical image-based 3D orthodontic wire optimization considering constraints at bracket and processing points. Med Biol Eng Comput 2025; 63: 3725-3733.
[30] Ganta GK, Mosca RC, Varsani R, Murthy VR, Cheruvu K, Lu M and Arany PR. Automation in dentistry with mechanical drills and lasers for implant osteotomy: a narrative-scoping review. Dent J (Basel) 2023; 12: 8.